H_2 Production by Selective Decomposition of Hydrous Hydrazine over Raney Ni Catalyst under Ambient Conditions

Lei He
State Key Laboratory of Catalysis, Dalian Institute of Chemical Physics, Chinese Academy of Sciences, Dalian, 116023, P. R. China

University of Chinese Academy of Sciences, Beijing, 100049, P. R. China

Yanqiang Huang, Aiqin Wang, Xiaodong Wang, and Tao Zhang
State Key Laboratory of Catalysis, Dalian Institute of Chemical Physics, Chinese Academy of Sciences, Dalian, 116023, P. R. China

DOI 10.1002/aic.14151
Published online June 25, 2013 in Wiley Online Library (wileyonlinelibrary.com)

A noble metal-free catalyst, Raney Ni, exhibited > 99% selectivity toward H_2 for hydrous hydrazine decomposition in basic solution at 30°C. The particle size of the initial Ni-Al alloy and the concentration of additional alkali influenced the H_2 selectivity on Raney Ni catalysts. This convenient route provides great potential for industrial application of hydrous hydrazine as a promising hydrogen storage material. © 2013 American Institute of Chemical Engineers *AIChE J*, 59: 4297–4302, 2013

Keywords: hydrous hydrazine decomposition, Raney Ni, hydrogen generation, alkali promotion

Introduction

Storing hydrogen safely and efficiently remains one of the major technological barriers preventing the large-scale utilization of hydrogen energy.[1] Chemical hydrogen storage is thought to be one of the most promising approaches to meet this challenge, due to its considerably high gravimetric and volumetric hydrogen density.[2–4] Recently, hydrous hydrazine, such as hydrazine monohydrate ($N_2H_4{\cdot}H_2O$), was discovered as a promising hydrogen carrier material for H_2 generation at ambient temperature, because it has the following advantages: high content of usable hydrogen (e.g., 8.0 wt % for $N_2H_4{\cdot}H_2O$), production of CO-free hydrogen by complete decomposition, and safe for handling.[5]

The decomposition of hydrazine proceeds via two typical reaction routes:

Complete decomposition

$$N_2H_4 \rightarrow N_2(g)+2H_2(g) \quad (1)$$

Incomplete decomposition

$$3N_2H_4 \rightarrow 4NH_3(g)+N_2(g) \quad (2)$$

Obviously, only the complete decomposition of hydrous hydrazine (pathway 1) led to H_2 generation and the pathway 2 should be hindered. However, it is a thermodynamic unfavorable process for complete decomposition of hydrazine (pathway 1) at low temperatures. For example, on the industrially used iridium catalyst for this process, the main products are NH_3 and N_2 at low temperatures, and the selectivity to H_2 is very low (~2%).[6,7] N—N bond is much easier to cleavage than N—H bond over Ir surface, which leads to the formation of NH_3 in the final products.[8] Thereby, it is a great challenge of developing efficient catalysts for the selective decomposition of hydrous hydrazine to H_2 production. To this end, a series of Ni-based bimetallic catalysts were synthesized, including Ni-Rh, Ni-Pt, and Ni-Ir, which showed alomost 100% H_2 selectivity at room temperature.[9–14]

Although these Ni-based bimetallic catalysts exhibited high selectivity to H_2, the cost of catalysts was greatly increased with the incorporation of noble metals. Thus, the development of completely noble metal-free catalysts is urgently required for selective decomposition of hydrous hydrazine. With this aim, Xu's group employed Ni-Fe nanoparticle as the catalyst, which exibited 100% selectivity to H_2 in basic solution when the temperature increased to 70 °C.[15] Shao and coworkers once reported that composite oxide $Ba_{0.5}Sr_{0.5}Co_{0.8}Fe_{0.2}O_{3-\delta}$ (BSCF) was an effective catalyst for the decomposition of liquid hydrazine to H_2 and N_2 in strong basic conditions.[16,17] Meanwhile, Tong et al. prepared Fe-B catalyst for hydrogen generation from the N_2H_4 decomposition.[18] In our recent work, a supported Ni/Al_2O_3 catalyst was synthesized using Ni-Al hydrotalcite as a precursor, which showed 93% selectivity to H_2 for this reaction at 30°C.[19] This unique catalysis is due to the cooperative action of highly dispersed metallic Ni particles and strong basic sites located in the neighborhood.

Previous research has indicated that, among all the metallic catalyst systems, Ni showed the highest selectivity to H_2 from hydrous hydrazine decomposition under mild conditions. Raney Ni is one of the most widely used Ni catalysts in industry due to its high activity, large BET surface area, and structural stability.[20–27] In this work, we have discovered that

Correspondence concerning this article should be addressed to T. Zhang at taozhang@dicp.ac.cn.

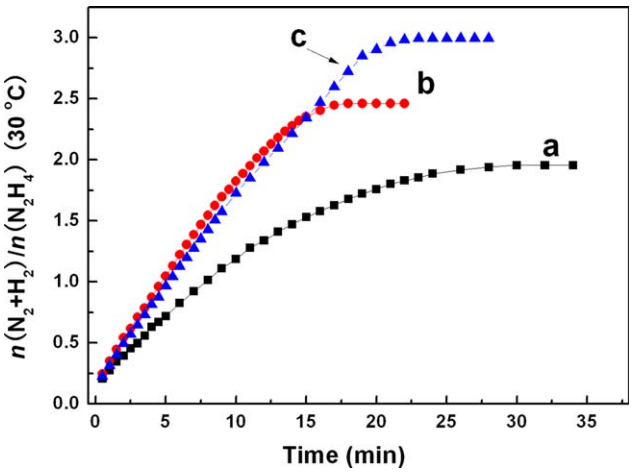

Figure 1. Kinetic plots for Raney Ni with different meshes (a) Raney Ni-40, (b) Raney Ni-300, and (c) Raney Ni-300 with addition of NaOH (0.5 mol L^{-1}).

The reaction temperature was 30°C. [Color figure can be viewed in the online issue, which is available at wileyonlinelibrary.com]

Raney Ni is both active and selective for H_2 production from hydrous hydrazine decomposition. This noble metal-free catalyst showed high (> 99%) and sustainable selectivity to H_2 in basic solution (NaOH solution) at 30°C. Separation of this catalyst from the reactant liquid is quite simple by using a magnet, as Raney Ni has an excellent magnetic property. This convenient route provides great potential for industrial application of hydrous hydrazine as a promising hydrogen storage material.

Experimental Procedure

Hydrous hydrazine decomposition test

Two types of commercialized Raney Ni catalysts were employed for hydrous hydrazine decomposition. They were denoted as Raney Ni-40 and Raney Ni-300, indicating that the original particle size of catalysts were 40 meshes and 300 meshes, respectively. The Raney Ni-40 and Raney Ni-300 were provided by Dalian General Chemical Industry Co., Ltd. Both catalysts were washed with degassed water before utilization.

The decomposition test was carried out in a three-necked round-bottom flask containing ~0.20 g Raney Ni with 5 mL oxygen-free water to avoid oxidation. When NaOH was necessary, it is dissolved in the water mentioned previously and cooled to reaction temperature before the test. Under magnetic stirring, the reaction was initiated by introducing 5 mL diluted hydrous hydrazine solution (containing 1.6 mmol N_2H_4) into the reactor. The gaseous product was allowed to pass through a trap containing 0.5 mol L^{-1} hydrochloric acid to ensure the absorption of ammonia, and was then measured volumetrically using the gas burette connected to one neck of the reactor.

The selectivity toward hydrogen generation (x) was evaluated on the basis of the equation: 3 $N_2H_4 \rightarrow$ 4(1-x) NH_3 + 6x H_2 + (1+2x) N_2, which could be deduced from the Eqs. 1 and 2 in this article. The selectivity is defined as follows

$$x = \frac{3\lambda - 1}{8}\left[\lambda = \frac{n(N_2 + H_2)}{n(N_2H_2)}\left(\frac{1}{3} \le \lambda \le 3\right)\right]$$

The turnover frequency (TOF) value was calculated as follows

$$\mathrm{TOF} = \frac{C}{m_{\mathrm{Ni}} \times D \times t}$$

C is 30% conversion of hydrous hydrazine (g), m_{Ni} is the mass of Ni in the catalyst (g), D is the metal dispersion, and t: reaction time (min).

Characterization

Thermo IRIS Intrepid II inductively coupled plasma (ICP) was used to determine the exact content of Ni and Al in Raney Ni-40 and Raney Ni-300 catalysts. The X-ray diffraction (XRD) patterns were recorded with a PANalytical X'Pert-Pro powder X-ray diffractometer, using Cu K_α monochromatized radiation ($\lambda = 0.1541$ nm) at a scan speed of 5° min^{-1}. The scanning angle (2θ) range was from 10° to 80°, operated at 40 kV and 40 mA. The SEM images were recorded using a HITACHI S-5500 FE—SEM instrument. Nitrogen adsorption−desorption measurements were performed at −196°C with a Micrometrics ASAP2010 instrument. The specific surface areas were calculated with BET equation(S_{BET}).

The metal dispersion of Raney Ni was measured by H_2 pulse adsorption method on a Micromeritics AutoChem II 2920 automated catalyst characterization system. The samples were first flushed with Ar for 2 h at 150°C to remove water in the catalysts. After cooling to 50°C, H_2 was injected until saturation. The amount of H_2 adsorbed could be calculated from the pulse results monitored by a thermal conductivity detector (TCD). The metal dispersion was obtained from the H_2 adsorption results by assuming adsorption of one H per Ni atom.

Results and Discussion

The Raney Ni-40 and Raney Ni-300 catalysts were tested in the hydrous hydrazine decomposition reaction. Figure 1 illustrated that both of the Raney Ni catalysts showed 100% conversion of hydrous hydrazine at 30°C. However, Raney Ni-300 exhibited 80% selectivity to H_2, which was higher than Raney Ni-40 (68%, Table 1). The N_2H_4 decomposition turnover frequency (TOF) was 2.0 min^{-1} on Raney Ni-300 at 30°C, which was also higher than that on Raney Ni-40 (1.1 min^{-1}, Table 1). The performance difference was probably attributed to the structural difference of the two types of Raney Ni catalysts. From XRD patterns (Figure 2), it is

Table 1. Summary of H_2 Selectivity and TOFs for Different Catalysts at 30°C

Catalyst	Raney Ni-40	Raney Ni-300	Raney Ni-300 + NaOH (0.5 mol L^{-1})	Raney Ni-300 + NaOH (0.5 mol L^{-1})−20th cycle
Selectivity (%)	68	80	>99	96
TOF[a] (min^{-1})	1.1	2.0	1.9	1.9

[a]TOF value was calculated at the conversion of 30%

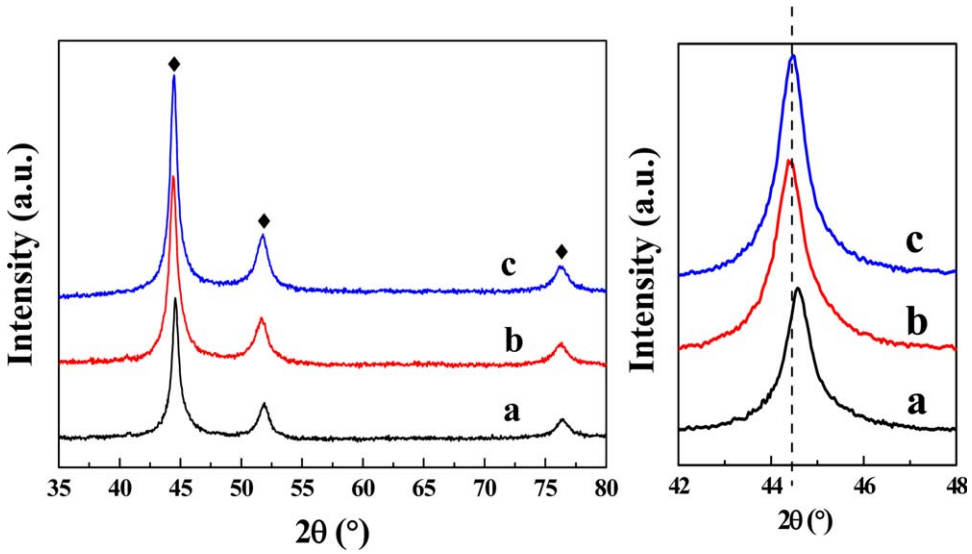

Figure 2. XRD patterns for (a) Raney Ni-40, (b) Raney Ni-300, and (c) Raney Ni-300 after 20 cycles of reaction.

Crystalline phase: (◆) metallic Ni. [Color figure can be viewed in the online issue, which is available at wileyonlinelibrary.com]

observed that the main diffraction peaks of Raney Ni-300 were at 44.4, 51.7, and 76.2°, which belonged to (111), (200), and (220) planes of fcc Ni (PDF #01–089-7128), respectively. However, the three peaks slightly shifted to higher angles (44.6, 51.9, and 76.4°) for Raney Ni-40. This little shift to higher angles may be attributed to the remaining Ni-Al alloy in Raney Ni-40 catalyst because of a smaller atomic radius for Al atom. Extraction of aluminum from Ni-Al alloy precursor is an important step in preparing Raney Ni catalyst, leaving behind a porous residue of nonsoluable Ni.[26,27] Compared with Raney Ni-300, the particle size of Ni-Al precursor was larger for Raney Ni-40, which may lead to more Al remaining in the final catalyst. ICP results indeed indicated that the contents of Al were higher in Raney Ni-40 (6.9 wt %) than in Raney Ni-300 (5.8 wt %) (Table 2). Figure 3 shows the HRSEM images of the studied catalysts. Both of the catalysts were constituted by fractured and stratified particles. This typical stratified structure was generated after leaching Al from the Ni-Al alloy precursor. However, compared with Raney Ni-40, the structure was more homogeneously distributed in Raney Ni-300 catalyst with a brighter border, indicating less Al residue.[21] Therefore, the size of the Ni-Al alloy precursor may have an influence on the aluminum extraction, which is easier to occur on the precursor with a smaller size, for example Raney Ni-300. Moreover, Al_2O_3 may be formed during the leaching process, which also makes it difficult for Al leaching from the inside of Ni-Al particles.[27] It has been reported that this remaining Al species could modify the chemisorption properties of reactant molecules.[28,29] The lower activity and selectivity on Raney Ni-40 reflects the detrimental effect of residue Ni-Al alloy, which prevents the selective activation of N—H bond. Hereafter, we focused our following study on Raney Ni-300 catalyst.

Table 2. ICP, Metal Dispersion and S_{BET} Results for Raney Ni-40 and Raney Ni-300

Catalyst	Ni (wt%)	Al (wt%)	Metal dispersion D (%)	S_{BET} ($m^2\ g^{-1}$)
Raney Ni-40	75.5	6.9	2.0	57
Raney Ni-300	74.8	5.8	2.1	55
Raney Ni-300 + NaOH (0.5 mol L^{-1})−20th cycle	77.9	3.7	-	32

To further improve the performance, alkali (NaOH) was used as a promoting additive to Raney Ni-300 catalyst in this reaction. It has been reported that the existence of strong basic sites plays an important role in promoting the selectivity to H_2.[15,16] The amount of additional NaOH was adjusted and precisely controlled. Interestingly, the selectivity to H_2 was promoted to 91% from the original 80%, when the concentration of NaOH solution was 0.05 mol L^{-1} (Figure 4). The selectivity was further raised by increasing the amount of additional NaOH. To be noted, the selectivity to H_2 reached > 99% when the concentration of NaOH solution was extended to 0.5 mol L^{-1}, and this high selectivity remained as further increasing the amount of NaOH. In other words, the addition of NaOH is beneficial for H_2 selectivity, which coincides well with the results reported over BSCF, Ni-Fe, and Rh-Ni/graphene catalysts.[13,15,16] The possible reason of this promoting effect will be discussed below.

We also measured the influence of reaction temperature on H_2 selectivity. As shown in Table 3, an increase in temperature is accompanied by an increase in reaction rate. It was found, however, the H_2 selectivity was gradually decreased with increasing reaction temperature. We calculated the apparent activation energy for each decomposition pathway over Raney Ni-300 catalyst before and after adding NaOH (Figure 5). The results showed that the variation of apparent activation energies for reactions (1) and (2) were quite different after adding NaOH as a promoter. For pathway 1, this value decreased from 47.5 ± 1.6 kJ mol^{-1} to 44.4 ± 1.7 kJ mol^{-1}, while increased from 60.5 ± 1.8 kJ mol^{-1} to 92.7 ± 4.1 kJ mol^{-1} for pathway 2. These data indicated that the addition of NaOH increased the energy barrier for NH_3 generation but scarcely influenced that for H_2 production. Consequently, when the two pathways competed with each other during the process of hydrous hydrazine decomposition, reaction was easier to occur toward pathway (1) after adding NaOH.

The aforementioned results have illustrated that the selectivity to H_2 on Raney Ni-300 catalyst was significantly promoted

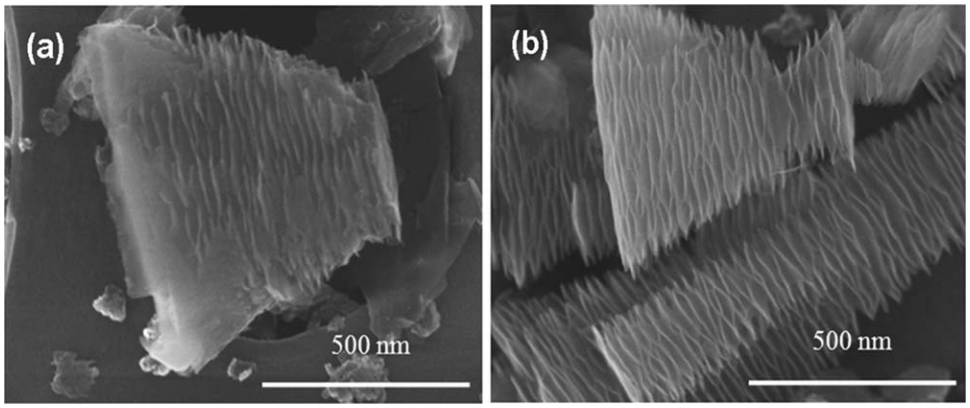

Figure 3. SEM images of (a) Raney Ni-40 catalyst, and (b) Raney Ni-300 catalyst.

to > 99% after adding NaOH. Alkali (e.g., NaOH) itself could not catalyze the decomposition of hydrous hydrazine. The additional alkali only played the role of a promoter for the enhanced selectivity. As the presence of NaOH provides OH^- in solution, which may create a strong basic environment, and, thereby, inhibit the production of basic NH_3 via incomplete decomposition (pathway 2). Besides, the decomposition of N_2H_4 contains several elemental reaction steps. It has been reported that the preferred cleavage of N—H bond instead of N—N bond leads to the complete decomposition of N_2H_4 to N_2 and H_2.[30,31] The break of first N—H bond ($N_2H_4 \rightarrow N_2H_3^* + H^*$) is thought to be a rate-determine step, which could be accelerated by adding alkali.[15,30] In addition, The existence of OH^- reduces the amount of $N_2H_5^+$, generated from ionization of N_2H_4 in water, which is beneficial for the reaction.

The reusability was evaluated for this effective catalyst system (Raney Ni-300 combined with NaOH). To be noted, as Raney Ni catalyst showed perfect magnetic property, the catalyst could be easily collected and reused after each cycle (Figure 6). Twenty cycles of reaction were carried out over the same Raney Ni-300 catalyst in basic solution (NaOH,

Table 3. Comparison of H_2 Selectivity and TOF for Raney Ni-300 with and without NaOH at Different Reaction Temperatures

Reaction Temperature (°C)	Raney Ni-300		Raney Ni-300 + NaOH[b]	
	Selectivity (%)	TOF[a] (min^{-1})	Selectivity (%)	TOF[a] (min^{-1})
30	80	2.9	>99	2.7
40	79	5.4	96	5.2
50	76	9.7	93	8.5
60	75	18.0	89	13.4
70	72	33.1	87	23.2
80	70	44.9	85	39.4

[a]TOF value was calculated at the conversion of 30 %.
[b]The concentration of NaOH was 0.5 mol L^{-1}.

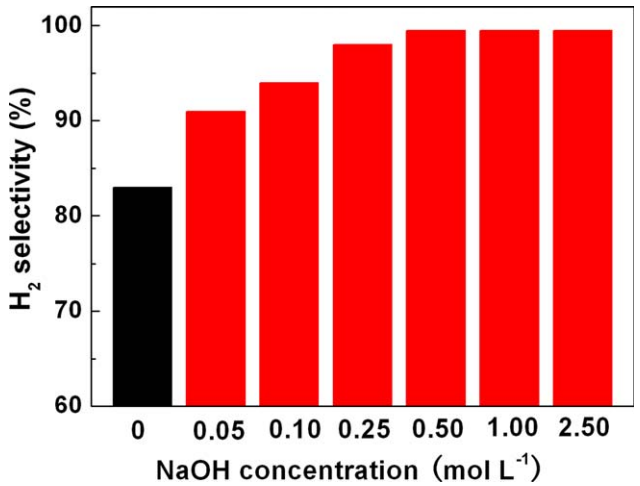

Figure 4. Comparison of H_2 selectivity in the decomposition of hydrous hydrazine (0.16 mol L^{-1}) catalyzed by Raney Ni with the addition of different amount NaOH.

The reaction was carried out at 30°C. [Color figure can be viewed in the online issue, which is available at wileyonlinelibrary.com]

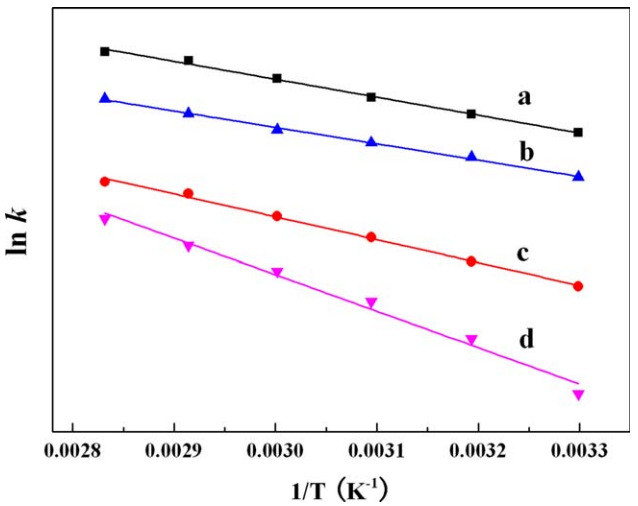

Figure 5. Kinetic plots and corresponding fitting lines for hydrous hydrazine decomposition over Raney Ni-300 with and without NaOH (0.5 mol L^{-1}) at 30–80°C: a, b. fitting lines for pathway (1) over Raney Ni-300 before and after adding NaOH; c, d. fitting lines for pathway (2) over Raney Ni-300 before and after adding NaOH.

[Color figure can be viewed in the online issue, which is available at wileyonlinelibrary.com]

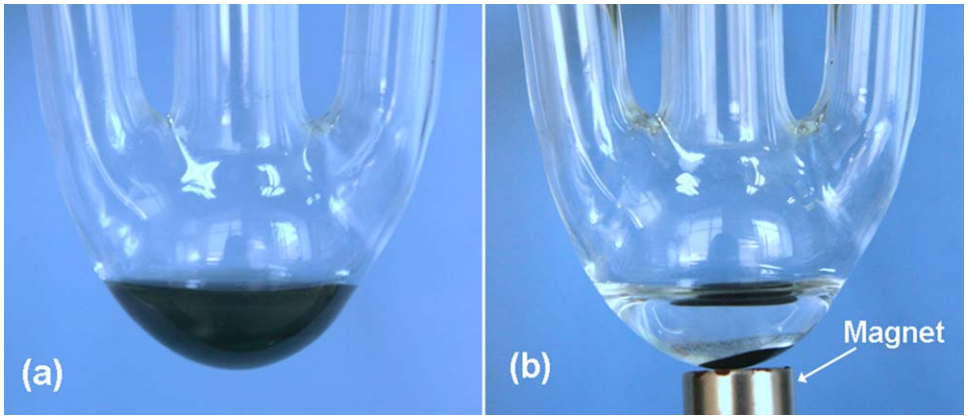

Figure 6. Magnetic separation property of Raney Ni-300 catalyst after each cycle of reaction (a) reactants with catalyst after reaction, and (b) with a magnet to separate catalyst.

[Color figure can be viewed in the online issue, which is available at wileyonlinelibrary.com]

0.5 mol L^{-1}) (Figure 7). The recycling test showed $\geq 99\%$ selectivity for this reaction during the first three cycles. For the next 17 cycles, the selectivity remained $\sim 97\%$ without obvious changes. Even after 20 cycles of reaction, this catalyst still showed as high as 96% selectivity to H_2. The XRD pattern of this Raney Ni-300 catalyst after 20 cycles was shown in Figure 2c. The position of diffraction peaks for Ni particles remained the same compared with the fresh Raney Ni-300 catalyst, but the intensity was slightly intensified. The size of Ni particle increased a little from 10.4 nm to 11.9 nm calculated by Sherrer equation. A few percentages of Al species were leached away after immersed in NaOH solution for 20 cycles of reaction (Table 2), which led to a slight increase of the Ni particle size. The leaching of Al also led to a decrease of surface area for Raney Ni-300 from 55 m^2 g^{-1} to 32 m^2 g^{-1}. However, the TOF and the H_2 selectivity over the Raney-Ni-300 remained almost the same values even after 20 cycles of activity test, indicating that the extraction of Al under reaction conditions has minor influence on the catalytic performance in this case.

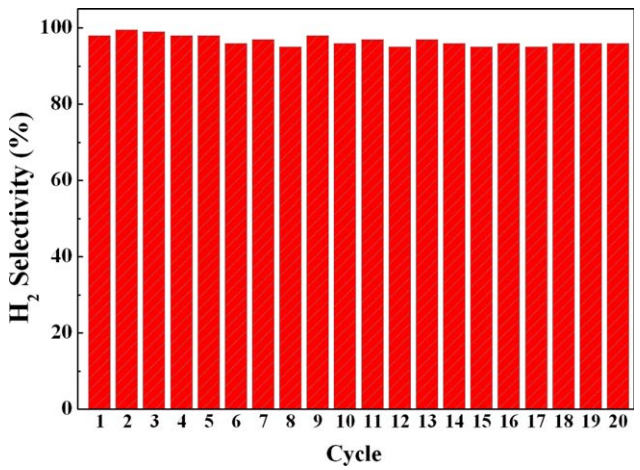

Figure 7. The recycling test of Raney Ni-300 with NaOH (0.5 mol L^{-1}) for hydrous hydrazine decomposition, carried out at 30°C.

[Color figure can be viewed in the online issue, which is available at wileyonlinelibrary.com]

Conclusion

Raney Ni catalyzed the decomposition of hydrous hydrazine with $> 99\%$ selectivity to H_2 after adding small amount of NaOH. Compared with Raney Ni-40, Raney Ni-300 exhibited higher activity and H_2 selectivity in this reaction, which was probably caused by the relatively lower content of remaining aluminum. NaOH played the role of an effective promoter for H_2 selectivity by hindering NH_3 generation. This catalyst system (Raney Ni-300 + NaOH), with an advantage of resuablity, performed sustainable selectivity after 20 cycles of reaction. The usage of the low-cost, easy-getting catalyst to realize the production of CO-free hydrogen under mild condition gives more confidence for the application of hydrous hydrazine as a hydrogen storage material.

Acknowledgment

This work was supported by the Natural Science Foundation of China (21076211, 21103173, 21176235). Thanks for Dalian General Chemical Industry Co., Ltd. of providing Raney Ni-40 and Raney Ni-300 catalysts as we needed.

Literature Cited

1. Schlapbach L, Züttel A. Hydrogen-storage materials for mobile applications. *Nature*. 2001;414:353–358.
2. Eberle U, Felderhoff M, Schüth F. Chemical and physical solutions for hydrogen storage. *Angew. Chem Int Ed*. 2009;48:6608–6630.
3. Yang J, Sudik A, Wolverton C, Siegel DJ. High capacity hydrogen storage materials: attributes for automotive applications and techniques for materials discovery. *Chem Soc Rev*. 2010;39:656–675.
4. Demirci UB, Miele P. Chemical hydrogen storage: 'material' gravimetric capacity versus 'system' gravimetric capacity. *Energy Environ. Sci*. 2011;4:3334–3341.
5. Jiang HL, Singh SK, Yan JM, Zhang XB, Xu Q. Liquid-phase chemical hydrogen storage: catalytic hydrogen generation under ambient conditions. *ChemSusChem*. 2010;3:541–549.
6. Zheng M, Cheng R, Chen X, Li N, Li L, Wang X, Zhang T. A novel approach for CO-free H_2 production via catalytic decomposition of hydrazine. *Int J Hydrogen Energy*. 2005;30:1081–1089.
7. Mary S, Kappenstein C, Balcon S, Rossignol S, Gengembre E. Monopropellant decomposition catalysts. I. Aging of highly loaded Ir/Al_2O_3 catalysts in oxygen and steam. Influence of chloride content. *Appl Catal A*. 1999;182:317–325.
8. Zhang P, Wang Y, Huang Y, Zhang T, Wu G, Li J. Density functional theory investigations on the catalytic mechanisms of hydrazine decompositions on Ir(111). *Catal Today*. 2011;165:80–88.
9. Singh SK, Xu Q. Complete conversion of hydrous hydrazine to hydrogen at room temperature for chemical hydrogen storage. *J Am Chem Soc*. 2009;131:18032–18033.

10. Singh SK, Xu Q. Bimetallic nickel-iridium nanocatalysts for hydrogen generation by decomposition of hydrous hydrazine. *Chem Commun*. 2010;46:6545–6547.
11. Singh SK, Xu Q. Bimetallic Ni-Pt nanocatalysts for selective decomposition of hydrazine in aqueous solution to hydrogen at room temperature for chemical hydrogen storage. *Inorg Chem*. 2010;49:6148–6152.
12. Singh SK, Lu ZH, Xu Q. Temperature-induced enhancement of catalytic performance in selective hydrogen generation from hydrous hydrazine with Ni-based nanocatalysts for chemical hydrogen storage. *Eur J Inorg Chem*. 2011;14:2232–2237.
13. Wang J, Zhang X, Wang Z, Wang L, Zhang Y. Rhodium-nickel nanoparticles grown on graphene as highly efficient catalyst for complete decomposition of hydrous hydrazine at room temperature for chemical hydrogen storage. *Energy Environ Sci*. 2012;5:6885–6888.
14. He L, Huang Y, Wang A, Liu Y, Liu X, Chen X, Delgado JJ, Wang X, Zhang T. Surface modification of Ni/Al_2O_3 with Pt: highly efficient catalysts for H_2 generation via selective decomposition of hydrous hydrazine. *J Catal*. 2013;298:1–9.
15. Singh SK, Singh AK, Aranishi K, Xu Q. Noble-metal-free bimetallic nanoparticle-catalyzed selective hydrogen generation from hydrous hydrazine for chemical hydrogen storage. *J Am Chem Soc*. 2011;133:19638–19641.
16. Song J, Ran R, Shao Z. Hydrazine as efficient fuel for low-temperature SOFC through ex-situ catalytic decomposition with high selectivity toward hydrogen. *Int. J. Hydrogen Energy*. 2010;35:7919–7924.
17. Zhao B, Song J, Ran R, Shao Z. Catalytic decomposition of hydrous hydrazine to hydrogen over oxide catalysts at ambient conditions for PEMFCs. *Int J Hydrogen Energy*. 2012;37:1133–1139.
18. Tong DG, Chu W, Wu P, Gu GF, Zhang L. Mesoporous multiwalled carbon nanotubes as supports for monodispersed iron-boron catalysts: improved hydrogen generation from hydrous hydrazine decomposition. *J Mater Chem A*. 2013;1:358.
19. He L, Huang Y, Wang A, Wang X, Chen X, Delgado JJ, Zhang T. A noble-metal-free catalyst derived from Ni-Al hydrotalcite for hydrogen generation from $N_2H_4{\cdot}H_2O$ decomposition. *Angew Chem Int Ed*. 2012;51:6191–6194.
20. Huber GW, Shabaker JW, Dumesic JA. Raney Ni-Sn catalyst for H_2 production from biomass-derived hydrocarbons. *Science*. 2003;300:2075–2077.
21. Zhang C, Zhang P, Li S, Wu G, Ma X, Gong J. Superior reactivity of skeletal Ni-based catalysts for low-temperature steam reforming to produce CO-free hydrogen. *Phys Chem Chem Phys*. 2012;14:3295–3298.
22. Yin A-Y, Guo X-Y, Dai W-L, Fan K-N. The synthesis of propylene glycol and ethylene glycol from glycerol using Raney Ni as a versatile catalyst. *Green Chem*. 2009;11:1514–1516.
23. Liu B, Qiao M, Deng J, K. Fan, Zhang X, Zong B. Skeletal Ni catalyst prepared from a rapidly quenched Ni-Al alloy and its high selectivity in 2-ethylanthraquinone hydrogenation. *J Catal*. 2001;204:512–515.
24. Lu L, Rong Z, Du W, Ma S, Hu S. Selective hydrogenation of single benzene ring in biphenyl catalyzed by skeletal Ni. *ChemCatChem* 2009;1:369–371.
25. Zong B, Zhang X, Qiao M. Integration of methanation into the hydrogenation process of benzoic acid. *AIChE J*. 2009;55:192–197.
26. Hu H, Qiao M, Wang S, Fan K, Li H, Zong B, Zhang X. Structural and catalytic properties of skeletal Ni catalyst prepared from the rapidly quenched $Ni_{50}Al_{50}$ alloy. *J Catal*. 2004;221:612–618.
27. Barnard NC, Brown SGR, Devred F, Bakker JW, Nieuwenhuys BE, Adkins NJ. A quantitative investigation of the structure of Raney-Ni catalyst material using both computer simulation and experimental measurements. *J Catal*. 2011;281:300–308.
28. Zhu LJ, Guo PJ, Chu XW, Yan SR, Qiao MH, Fan KN, Zhang XX, Zong BN. An environmentally benign and catalytically efficient nonpyrophoric Ni catalyst for aqueous-phase reforming of ethylene glycol. *Green Chem*. 2008;10:1323–1330.
29. Freel J, Robertson SD, Anderson RB, The structure of Raney nickel: III. The chemisorption of hydrogen and carbon monoxide. *J Catal*. 1970;18:243–248.
30. Rosca V, Duca M, Groot MT, Koper MTM. Nitrogen Cycle Electrocatalysis. *Chem Rev*. 2009;109:2209–2244.
31. Alberas DJ, Kiss J, Liu ZM, White JM. Surface chemistry of hydrazine on Pt(111). *Surf Sci*. 1992;278:51–61.

Manuscript received Feb. 6, 2013, and revision received Apr. 2, 2013.